

Adipose-Derived Stem Cells Enhance Axonal Regeneration through Cross-Facial Nerve Grafting in a Rat Model of Facial Paralysis

Ozan L. Abbas, M.D.
Hüseyin Borman, M.D.
Çağrı A. Uysal, M.D.
Zeynep B. Gönen
Leyla Aydın, D.D.S, Ph.D.
Fatma Helvacıoğlu, Ph.D.
Şebnem İlhan, M.D.
Ayşe C. Yazıcı, Ph.D.

Kırşehir, Ankara, and Kayseri, Turkey



Background: Cross-face nerve grafting combined with functional muscle transplantation has become the standard in reconstructing an emotionally controlled smile in complete irreversible facial palsy. However, the efficacy of this procedure depends on the ability of regenerating axons to breach two nerve coaptations and reinnervate endplates in denervated muscle. The current study tested the hypothesis that adipose-derived stem cells would enhance axonal regeneration through a cross-facial nerve graft and thereby enhance recovery of the facial nerve function. **Methods:** Twelve rats underwent transection of the right facial nerve, and cross-facial nerve grafting using the sciatic nerve as an interpositional graft, with coaptations to the ipsilateral and contralateral buccal branches, was carried out. Rats were divided equally into two groups: a grafted but nontreated control group and a grafted and adipose-derived stem cell-treated group. Three months after surgery, biometric and electrophysiologic assessments of vibrissae movements were performed. Histologically, the spectra of fiber density, myelin sheath thickness, fiber diameter, and g ratio of the nerve were analyzed. Immunohistochemical staining was performed for the evaluation of acetylcholine in the neuromuscular junctions.

Results: The data from the biometric and electrophysiologic analysis of vibrissae movements, immunohistochemical analysis, and histologic assessment of the nerve showed that adipose-derived stem cells significantly enhanced axonal regeneration through the graft.

Conclusion: These observations suggest that adipose-derived stem cells could be a clinically translatable route toward new methods to enhance recovery after cross-facial nerve grafting. (*Plast. Reconstr. Surg.* 138: 387, 2016.)

Facial nerve injuries encompass a broad spectrum of dysfunctions, ranging from subtle dynamic facial asymmetry to complete, dense paralysis.¹ Disabilities encountered include

corneal exposure, oral incompetence, and articulation difficulties.² None of these is perhaps as significant as the social isolation these patients often succumb to based on their perceived disfigurement and inability to convey emotion through facial expression.³ Because of the profound effect

From the Department of Plastic, Reconstructive, and Aesthetic Surgery, Ahi Evran University, Faculty of Medicine; the Departments of Plastic, Reconstructive, and Aesthetic Surgery, Physiology, Histology and Embryology, and Biostatistics, Başkent University, Faculty of Medicine; the Genome and Stem Cell Center, Stem Cell Unit, and the Department of Oral and Maxillofacial Surgery, Erciyes University, Faculty of Dentistry. Received for publication January 8, 2016; accepted March 17, 2016.

Presented at the Third European Association of Plastic Surgeons Research Council, in Isle of Ischia, Italy, May 28 through 29, 2014; and the 36th Annual Congress of the Turkish Plastic Reconstructive and Aesthetic Surgery Association, in Istanbul, Turkey, October 29 through November 1, 2014, and awarded second place in the best experimental study competition.

Copyright © 2016 by the American Society of Plastic Surgeons

DOI: 10.1097/PRS.0000000000002351

Disclosure: *The authors have no financial interest or other relationship with the manufacturers of any products or providers of any service mentioned in this article.*

Supplemental digital content is available for this article. Direct URL citations appear in the text; simply type the URL address into any Web browser to access this content. Clickable links to the material are provided in the HTML text of this article on the *Journal's* Web site (www.PRSJournal.com).

of this disorder on patient quality of life, a great deal of effort has been focused on reanimation of the paralyzed face.⁴

Patients with long-term facial paralysis are often reanimated with a two-stage procedure combining cross-facial nerve grafting with micro-neurovascular muscle transfer.⁵ The major disadvantage with cross-facial nerve grafting is that the results are inconsistent. Although some surgeons report excellent recovery,^{6–8} many others find it entirely unsatisfactory. The leading cause of failure is suspected to be poor traversing of motor axons from the contralateral facial nerve branches into, across, and eventually out of the nerve graft.⁹

Axonal regeneration through the graft is vigorously supported by a large number of trophic factors expressed locally.¹⁰ However, prolonged denervation and poor vascularization render the local environment unreceptive for axonal regeneration. For this reason, it is a logical approach to support the graft environment by replacing host cells with those derived exogenously. In the few past years, adipose tissue has been identified as possessing a population of multipotent adult stem cells to which we assign the generic nomenclature, adipose-derived stem cells.¹¹ Adipose-derived stem cells are an attractive cell source for tissue regeneration because of their self-renewal ability, high growth rate, and multipotent differentiation properties.¹² In addition, they can be isolated easily by a safe and conventional liposuction procedure from subcutaneous fat tissue.

Several studies have focused on different guidance conduits containing adipose-derived stem cells, which significantly enhanced nerve regeneration,^{13,14} and this effect has been attributed primarily to the environmental support provided by the adipose-derived stem cells during regeneration. Adipose-derived stem cells have also demonstrated the ability to promote angiogenesis, neurotrophic factor provision, and protection of neurons.¹⁵ Based on these reports, we aimed to provide functional benefits for axons traversing a cross-face nerve autograft by seeding the local environment with adipose-derived stem cells in a model of facial paralysis.

MATERIALS AND METHODS

Animals and Overview of the Study

This study was approved by the Baškent University Ethical Committee for Experimental Research on Animals. Twelve male Sprague-Dawley rats underwent cross-facial nerve grafting after

transection of the right main trunk of the facial nerve. Animals were subdivided into two groups according to the nature of injection; animals in the treatment group ($n = 6$) received 10^6 adipose-derived stem cells along the graft and suture lines. In contrast, animals in the control group ($n = 6$) received control medium. All assessments were made 90 days after surgery.

Isolation of Rat Adipose-Derived Stem Cells

Approximately $1 \times 1 \text{ cm}^3$ periperitoneal adipose tissue was harvested. Adipose tissue was washed in phosphate-buffered saline containing 1% penicillin-streptomycin solution (Biological Industries, Kibbutz Beit Haemek, Israel). Tissue samples were digested enzymatically in phosphate-buffered saline (Biological Industries) with 2.5 mg/ml collagenase type 2 (Sigma-Aldrich, Taufkirchen, Germany) for 30 minutes at 37°C. The cell suspension was filtered through a 70- μm cell strainer (Becton, Dickinson and Co., Franklin Lakes, N.J.) to separate cells from debris and undigested adipose tissue fragments. Cells were seeded into a 25-cm² culture flask containing standard culture medium (Dulbecco's Modified Eagle Medium) supplemented with 10% phosphate-buffered saline, 1% penicillin-streptomycin solution, and 1% stable glutamine (Biological Industries). The flasks were cultured in an incubator at 37°C and 5% carbon dioxide. After 3 days of first culture, the medium was refreshed and subsequently replaced twice a week. Adipose-derived stem cells were isolated on the basis of their adhesiveness to the culture plates. After cells reached 70 to 80% confluence in primary cell culture, cells were detached by 0.025% trypsin–ethylenediaminetetraacetic acid. The cells were washed with phosphate-buffered saline and replated at a 1:4 ratio for subculture. Adipose-derived stem cells from passage 3 were used for study.

Characterization of Adipose-Derived Stem Cells by Flow Cytometry

Undifferentiated adipose-derived stem cells were subjected to flow cytometric analyses for confirming that adipose-derived stem cells maintain their phenotypic characteristics in vitro. After passage 3, cells were harvested, centrifuged, and resuspended in phosphate-buffered saline at a concentration of 10^6 cells/ml. Immunophenotyping characterization of adipose-derived stem cells was performed with antibodies against the following human antigens: CD11b/c, CD29, CD44, CD45, CD73, and CD90. All antibodies were from

BD Biosciences. Flow cytometry was performed by using Navios (Beckman Coulter, Brea, Calif.). The data were analyzed with Kaluza software (Beckman Coulter). More than 50 percent staining was regarded as positive.

Count and Viability Assay

Viable cells were detected by using dual fluorescent probes of the Muse Count & Viability Assay kit (Merck, Millipore, Darmstadt, Germany) on a flow cytometer (Muse EasyCyte; Merck, Millipore).

Surgical Procedure

Each animal was anesthetized with an intraperitoneal injection of 50 mg/kg ketamine hydrochloride (Alfamine 10%; Alfasan, Woerden, Holland) and 10 mg/kg xylazine (Rompun 2%; Bayer, Leverkusen, Germany). The entire left sciatic nerve was harvested from close to the spinal cord to the distal lower extremity. The graft was then placed in saline, and an apron incision from auricle to auricle was made in the neck. The main trunk of the facial nerve was exposed bilaterally, and identification of the branches was then carried out using a nerve stimulator. On the right side, the main nerve trunk was transected, producing facial paralysis. On the same side, a 0.5-cm portion of the buccal branch was transected and removed. The graft was then reversed and coapted to the distal stump of the transected buccal branch using three 10-0 nylon sutures. On the contralateral side, the buccal branch was transected. The nerve graft was draped across the neck and coapted to the proximal stump of the transected left buccal

branch (Fig. 1). Animals in the treatment group received 1 cc of phosphate-buffered saline mixed with 10^6 adipose-derived stem cells around the graft and suture lines using a 1-cc syringe with a 26-gauge needle. In contrast, animals in the control group received 1 cc of phosphate-buffered saline.

Analysis of Vibrissae Motor Performance

In intact animals, two whisker movements are evident being large-amplitude vibrissal sweeps through protraction and retraction cycles. In both groups, all vibrissae of the right side acquired caudal orientation and remained motionless after transection of the facial nerve. The changes in whisking behavior after cross-facial nerve grafting were studied on postoperative day 90,¹⁶ and the values were compared with those obtained before surgery. To this end, one large vibrissa of the right side was used for biometric analysis. Under light anesthesia, all other vibrissae were clipped, and the animals were inserted into a custom-made restrainer for 20 minutes to pacify them. Using a Canon EOS 60D digital camera (Canon, Inc., Tokyo, Japan), video images of whisking behavior were captured. Captured video sequences were reviewed, and 2-second sequence fragments from each animal were selected. The stable position of the head, the frequency of whisking, and the degree of protraction were considered as selection criteria. Each vibrissa in this spatial model was represented by two points; its base and the point on the shaft 0.5 cm away from the base. The following parameters were evaluated: (1) protraction measured by the rostrally opened angles between the

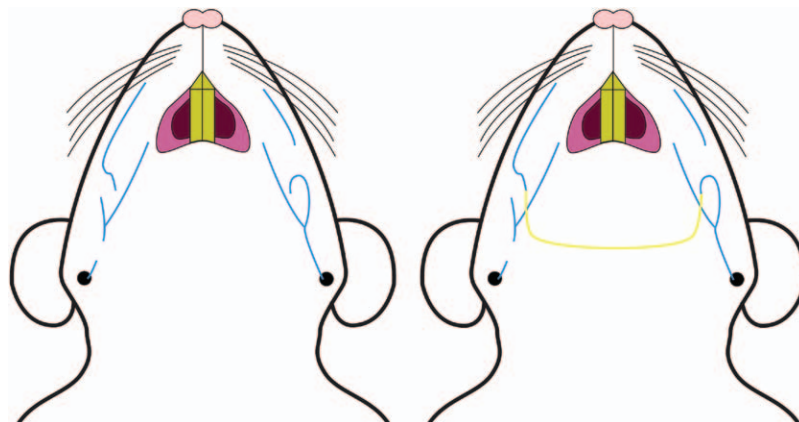


Fig. 1. (Left) The right main nerve trunk was transected, producing facial paralysis. On the same and contralateral sides, a 0.5-cm portion of the buccal branch was transected and removed. (Right) The nerve graft was then coapted to the distal stump of the transected right buccal branch and to the proximal stump of the transected left buccal branch.

midsagittal plane and the hair shaft (accordingly, maximal protractions were represented by rather low angle values); (2) the frequency of whisking (i.e., cycles of protraction and retraction per second); and (3) the amplitude (i.e., the difference between maximal retraction and maximal protraction in degrees).

Electromyographic Analysis

After induction of anesthesia, anodal and cathodal needle electrodes were inserted transcutaneously into the right vibrissal muscles. A reference needle electrode was inserted into the sternocleidomastoid muscle. Bipolar electrical stimulation was performed over the left buccal branch of the facial nerve. The intervals between stimulation for each recording were random, within a range of 3 to 10 seconds. Electrically evoked electromyograms were obtained using the MP36 system (BIOPAC Systems, Inc., Goleta, Calif.).

Histologic Assessment of the Nerve

The entire nerve graft, including the proximal and distal coaptation sites, was removed and segments were taken from specific sites. Site A was from the left buccal branch, site B was from the proximal sciatic nerve graft, and site C was from the distal sciatic nerve graft. These specimens were placed overnight in fixative, washed in buffer, fixed further in osmium tetroxide, dehydrated, and embedded in plastic resin. Then, 1- μ m-thick sections were cut and stained with toluidine blue. The mean number of myelinated axons per group was determined using a total magnification of 450 \times .

Assessment of myelination was performed by calculating the g ratio. This ratio was defined as the ratio of the axonal diameter divided by the diameter of the axon and its myelin sheath, and provides a structural and functional index of what might be considered as optimal axonal myelination. For the sciatic nerve, a g ratio between 0.55 and 0.68 was considered to be optimal.¹⁷ To calculate the g ratio, digitalized images of fiber cross-sections were obtained from site B. The g ratio was determined on at least 100 randomly chosen fibers per animal.

Immunohistochemical Analysis of Neuromuscular Junctions

Neuromuscular junctions were evaluated immunohistochemically using polyclonal anti-vesicular acetylcholine transporter primary antibodies (Abcam, Cambridge, United Kingdom).

The right buccal muscles were removed with the buccal branch attached. The muscle segment that contains the region of innervation was used for immunohistochemistry. Specimens were fixed for 1 hour in 4% paraformaldehyde in phosphate-buffered saline. Tissue was treated overnight with blocking serum. All primary antibodies were applied overnight in blocking serum and phosphate-buffered saline at 4°C. Slides were then rinsed for 30 minutes in phosphate-buffered saline, and the secondary antibody was administered in phosphate-buffered saline for 1 hour.

Statistical Analysis

Homogeneity of groups' variances was checked by the Levene test. Compliance with the normal distribution of continuous variables was checked with the Shapiro-Wilk test. When parametric test assumptions are available, two independent group means were compared by the *t* test. If assumptions are not available, the Mann-Whitney *U* test was used for comparisons of groups' medians. Dependent groups were analyzed by factorial repeated measures analysis of variance. Data analyses were performed using SPSS Version 17.0 (SPSS, Inc., Chicago, Ill.). A value of $p < 0.05$ was recognized as statistically significant.

RESULTS

Characterization of Adipose-Derived Stem Cells by Flow Cytometry

The adipose-derived stem cells isolated from rat adipose tissue were large and flattened and had a fibroblast-like shape. No significant morphologic changes were detected throughout the passages. The flow cytometric analysis data indicated that the cells expressed some commonly accepted mesenchymal stem cell markers such as CD29, CD44, CD73, and CD90. [See **Figure, Supplemental Digital Content 1**, which shows representative flow cytometric analyses of cell-surface markers in adipose-derived stem cells at passage 3. Adipose-derived stem cells expressed mesenchymal stem cell markers, including CD29 (91.7 percent), CD44 (90.4 percent), CD73 (90 percent), and CD90 (92.7 percent), but were negative for CD11b/c (4.7 percent) and CD45 (0.9 percent), <http://links.lww.com/PRS/B779>.] Viability was quantified by flow cytometric analysis after staining with count and viability kit before application, and 92.6 percent live cells were detected. (See **Figure, Supplemental Digital Content 2**, which shows viability quantification after staining with

the viability kit; 92.6 percent viable cells were detected, <http://links.lww.com/PRS/B780>.)

Analysis of Vibrissae Motor Performance

Before facial nerve transection, vibrissal motion was in the form of highly coordinated whisking with a frequency of approximately 6 Hz. The maximal protraction was approximately 60 degrees. The mean amplitude of whisking measured approximately 54 degrees. In the control group, large functional deficiency was evident from the significantly larger angle at maximal protraction (84 ± 4 degrees) and the smaller amplitude of vibrissae movement (17 ± 3 degrees) ($p < 0.001$). The frequency of movements was similar to intact animals. In contrast, all animals that received adipose-derived stem cells showed a significantly ($p < 0.001$) better recovery of the biometric parameters

compared with the animals in the control group (maximum angle of protraction, 77 ± 3 degrees; amplitude, 30 ± 4 degrees) (Fig. 2).

Electromyographic Analysis

The mean compound muscle action potential amplitude of the adipose-derived stem cell-treated group (5.37 ± 0.65 mV) was significantly higher ($p < 0.001$) than that of the control group (3.11 ± 1.21 mV). The mean compound muscle action potential duration of the treatment group (4.53 ± 0.37 msec) was significantly shorter ($p < 0.05$) in comparison with that of the control group (5.03 ± 0.57 msec). With respect to compound muscle action potential latencies, there was no significant difference between values recorded in both treatment (2.02 ± 0.20 mV) and control (1.85 ± 0.35 mV) groups. Significantly higher

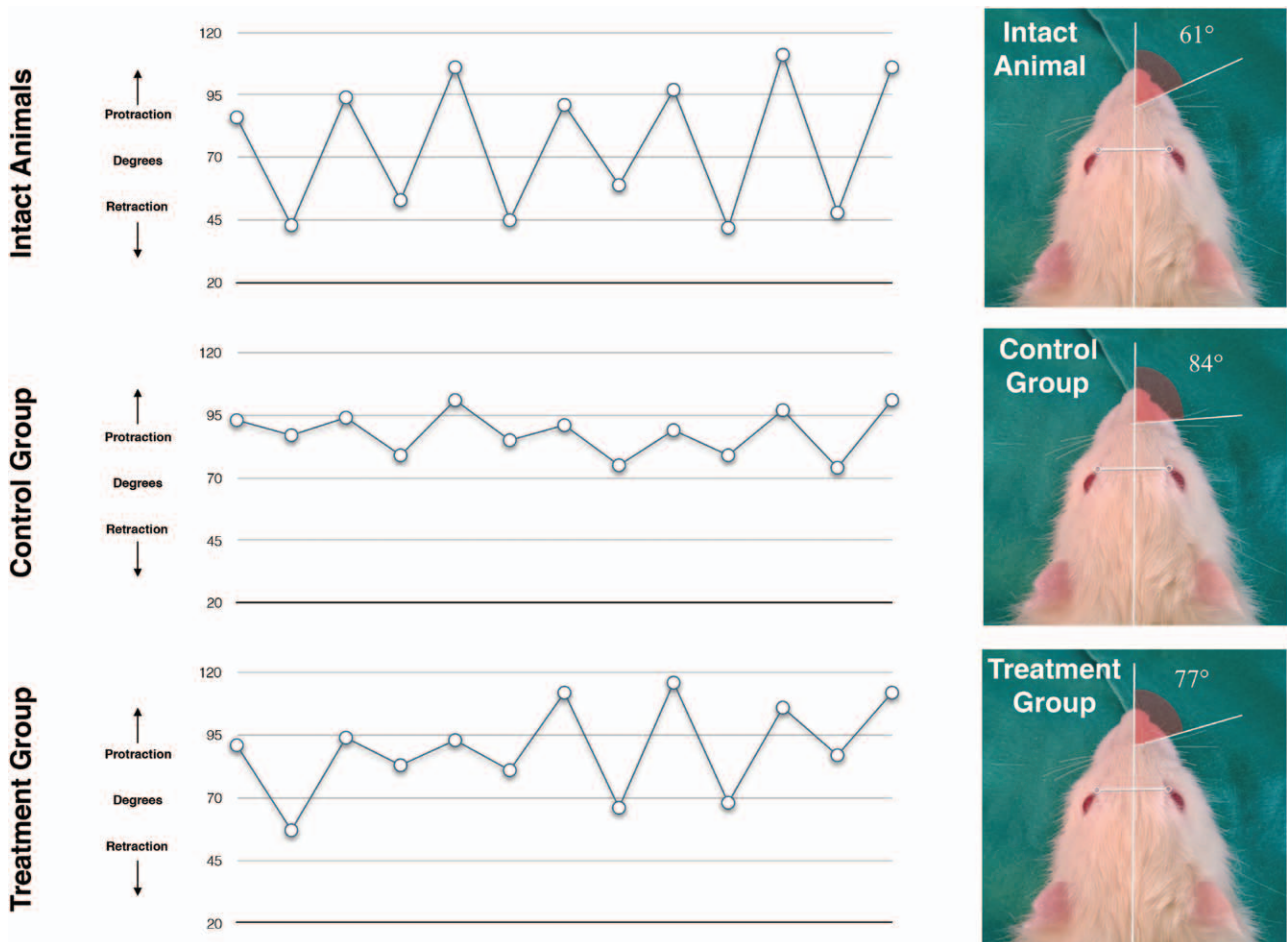


Fig. 2. Graphs of the changes in angles of the vibrissae during explorative cyclic whisking. (Above) In this case of an intact animal, the frequency was 5 Hz, the protraction was 61 degrees, and the amplitude was 50 degrees. (Center) Faint whisker movements during an active exploration of a representative animal 3 months after cross-facial nerve grafting only. (Below) Movement of a large vibrissa with a frequency of 5 Hz, a protraction of 73 degrees, and an amplitude of 29 degrees in a representative animal 3 months after cross-facial nerve grafting and adipose-derived stem cell application.

($p < 0.05$) threshold levels were obtained in the adipose-derived stem cells–treated group (1.07 ± 0.26 V) in comparison with the control group (0.63 ± 0.18 V) (Fig. 3).

Histologic Assessment of the Nerve

Mean axon counts from the selected cross-facial nerve grafting sites for the two groups are depicted graphically in Figure 4. In both groups, the mean numbers of axons in segment A were not statistically significantly different. In the control group, the mean number of axons in segment B was more than double the mean number of axons in segment A. However, statistical analysis failed to reveal a significant difference between the two segments. In the treatment group, the mean number of axons just distal to the proximal coaptation, segment B, was approximately three-fold greater than that just proximal to the coaptation. This difference was statistically significant ($p < 0.05$). In both groups, fewer axons were counted in segment C than in segment B. Statistical analyses revealed that these declines in axon numbers from the proximal portion to the distal portion of the graft were not significant. The mean number of axons in segment C of the treatment group was significantly greater than the mean number of axons in segment C of the control group ($p < 0.05$). Morphometric analysis did not show significant differences in terms of fiber size between both groups.

A mean g ratio of 0.62, which lies within the optimal range for the sciatic nerve, was obtained for nerve fibers of the treatment group. In contrast, the mean g ratio of the control group (0.49) was below the optimal range (Fig. 5). The difference between the two groups was statistically significant ($p < 0.001$).

Immunohistochemical Analysis of Motor Endplates

Immunohistochemical staining results with anti-vesicular acetylcholine transporter antibodies revealed different staining patterns with tissues obtained from both groups. Focal and weak expression of vesicular acetylcholine transporter molecules was detected in the neuromuscular junctions of adipose-derived stem cell–treated animals. In contrast, no expression was observed in tissues of the control group (Fig. 6).

DISCUSSION

The biometrics of whisking behavior provides a sensitive analysis tool with which to study facial nerve regeneration.¹⁶ Under normal physiologic conditions, the vibrissae of the rat are erect, with anterior orientation. Their simultaneous sweeps, known as whisking, occur five to 10 times per second.¹⁸ The striated muscle fibers that mediate protraction form a sling around the rostral aspect

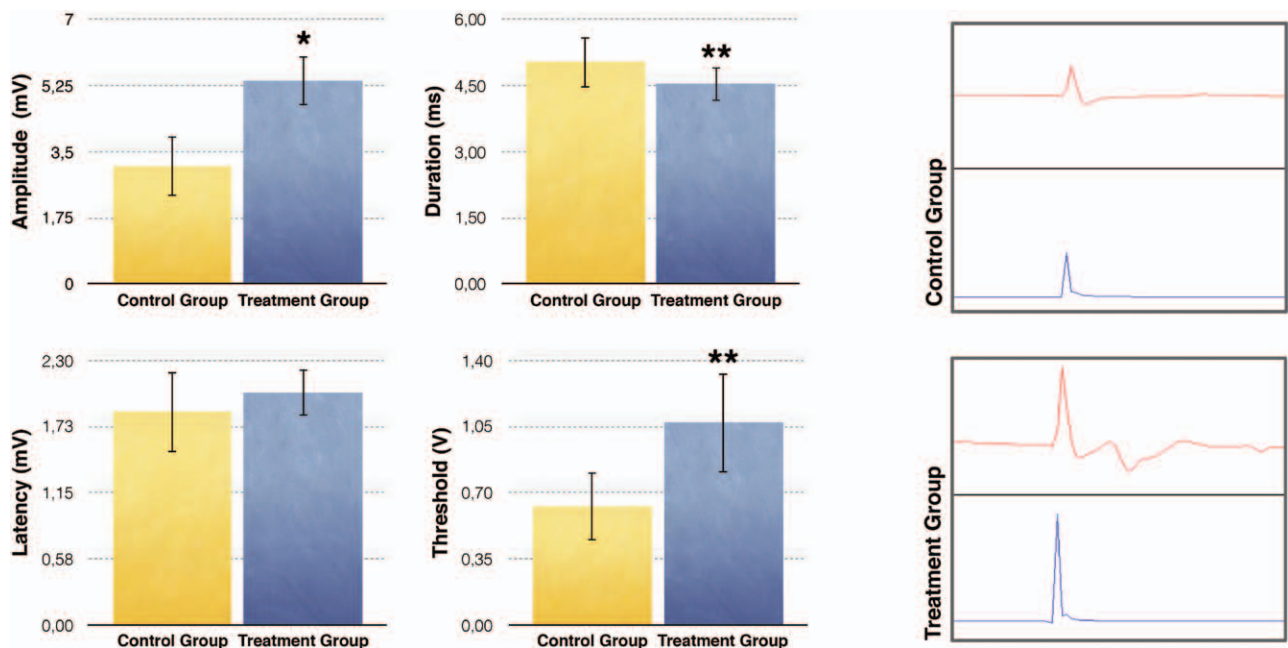


Fig. 3. (Left) Compound muscle action potential comparisons between two groups identified significant differences in the values of amplitude, duration, and threshold (* $p < 0.001$, ** $p < 0.05$). (Right) Representative recordings of compound muscle action potentials in control and adipose-derived stem cell–treated animals.

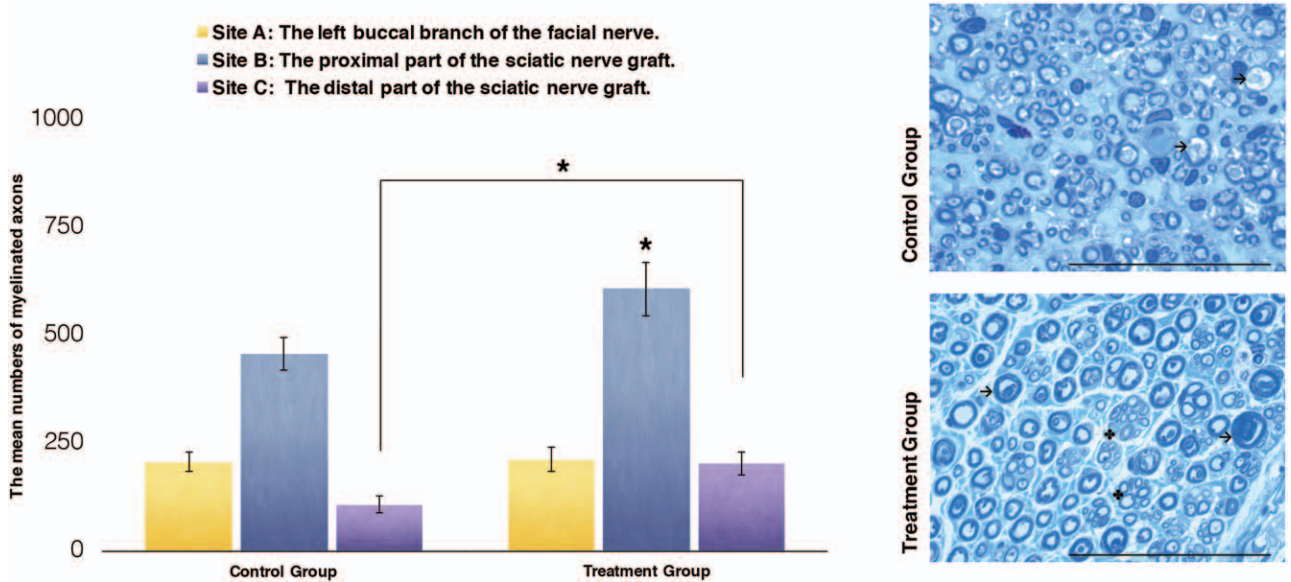


Fig. 4. (Left) Graphic comparisons of mean numbers of myelinated axons per segment of the nerve. (Right) Transverse sections of the sciatic nerve graft. Note that no significant regenerating units are seen in the control group. There are a few large myelinated fibers with irregular myelin (arrows) suggestive of atrophy. However, there are small thinly myelinated fibers (♣) and several large myelinated fibers with highly irregular myelin (arrows) in the treatment group, indicating regeneration and atrophic changes, respectively. Scale bar = 50 μ m.

of each hair follicle; contraction of these muscles by means of the buccal branch of the facial nerve pulls the base of the follicle caudally, moving the distal aspects of the whisker hair forward. By contrast, retraction of the vibrissae depends primarily on passive elastic properties of deep connective tissue.¹⁹ In this study, the role of adipose-derived stem cells in the functional outcome of cross-facial nerve grafting was shown dramatically by the return of more “normal” whisking, with greater range of motion.

Electrophysiologic assessment showed that higher compound muscle action potential amplitudes were recorded in the adipose-derived stem cell-treated group in comparison with the control group. Because compound muscle action potential amplitudes reflect the number of innervated muscle fibers,²⁰ these data are consistent with our vibrissal movement data and suggest that adipose-derived stem cell treatment influences the functional outcome of cross-facial nerve grafting. In contrast, the duration of compound muscle action potentials was shorter in animals in the treatment group, demonstrating that there was a better synchronization of the fibers in this group, resulting in improved function. The threshold value can vary according to numerous factors, such as fiber diameter and myelin thickness.²¹ Because motor nerves are composed of myelinated type A fibers with a diameter of 1 to 20 μ m,²² higher thresholds

in the treatment group show that regeneration occurred mainly in small-diameter fibers.

Axon counts from the different segments of the nerve provided evidence that administration of adipose-derived stem cells significantly increases the number of axons that enter the nerve graft. These data suggest the possibility that adipose-derived stem cells exerted their greatest influence on axonal sprouting and subsequent growth through the coaptation between the facial nerve and the nerve graft. In the treatment group, there were nearly three times as many axons in the nerve graft just distal to the proximal coaptation. These data suggest that adipose-derived stem cell administration caused each severed axon in the buccal branch of the facial nerve to give rise to an average of nearly three daughter axons that crossed the proximal coaptation site. The current data suggest further that adipose-derived stem cells may, in some way, inhibit the connective tissue reaction at the coaptation site, and thereby allow significantly more daughter axons to breach this region. There is another interesting set of data from the current study showing a significantly greater number of axons in the distal portion of the nerve graft in rats treated with adipose-derived stem cells. More axons not only breached the proximal coaptation but also arrived at the distal end of the nerve graft.

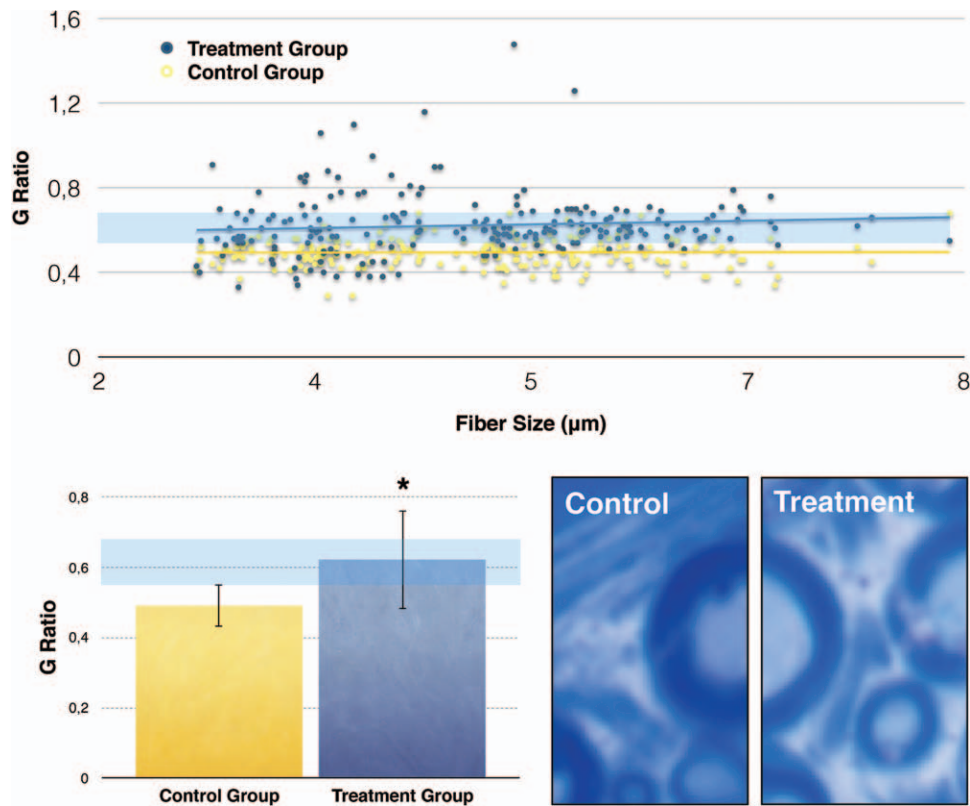


Fig. 5. (Above) The g ratio is consistently reduced in the control group (yellow) compared with the adipose-derived stem cell–treated group (blue) for virtually all axon diameters. (Below, left) The mean g ratio of adipose-derived stem cell–treated fibers (0.62) was within the optimal range for the sciatic nerve. In contrast, the mean g ratio of the control group (0.49) was below the optimal range. (Below, right) Electron micrographs depicting a single sciatic nerve fiber in both groups. Note that the myelin thickness is matched to axon diameter in the adipose-derived stem cell–treated group ($*p < 0.001$). The blue area indicates the optimal range of the g ratio for the sciatic nerve.

It is a widely held view that the g ratio is a highly reliable ratio for assessing axonal myelination.²³ In the treatment group, irrespective of fiber diameter, the myelin thickness is matched to axon diameter so that g ratios fall within the optimal range. As g ratios can be affected by the pathologic shrinkage of axonal caliber, we evaluated the distribution of axon size, and we did not find any difference between the two groups, suggesting that the ratio differed according to the thickness of myelin sheath.

One of the major requirements for optimal functional recovery after cross-facial nerve grafting is that the regenerating axons make functional connections with their muscle fibers. In the adipose-derived stem cell–treated animals, we confirmed the presence of acetylcholine in the neuromuscular junctions with immunohistochemistry. Besides being the main excitatory neurotransmitter in the peripheral nervous system, acetylcholine is capable of inducing neurite

outgrowth and promoting the formation of synapses.²⁴ Moreover, it has been shown that acetylcholine can control Schwann cell development and differentiation.²⁵ This dual role of acetylcholine may have contributed to functional outcomes of this study.

In this study, all assessments were performed 90 days after surgery. This period was planned, taking into consideration the rate of axonal regeneration. In rats, the rate of axonal regeneration has been assumed to be constant and is generally estimated to be 3 mm/day.²⁶ Therefore, all axotomized rat sciatic motoneurons would require approximately 17 days to regenerate their axons a distance of 50 mm. In addition, Gordon et al. documented that a period of 4 weeks is required for regenerating axons to cross a surgical suture site.²⁷ For this reason, the time required for regenerating axons to cross two suture lines and traverse a nerve graft up to 5 cm in length was calculated to be 3 months.

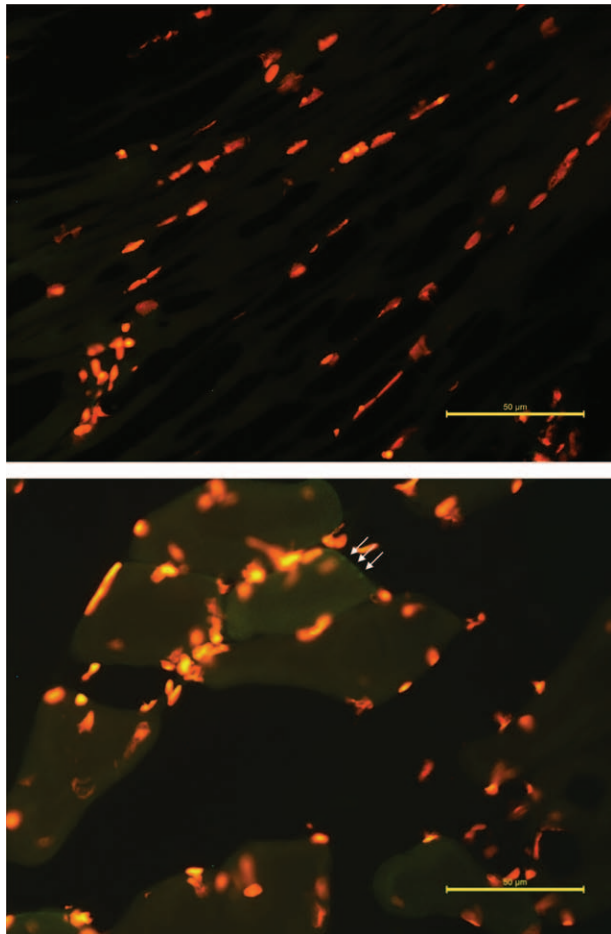


Fig. 6. (Below) Focal expression of vesicular acetylcholine transporter molecules was located in the neuromuscular junctions of adipose-derived stem cell-treated animals (arrows). (Above) In contrast, no expression was observed in tissues of the control group. Scale bar = 50 µm.

Our findings indicate that adipose-derived stem cells act through multiple mechanisms to benefit animals with facial paralysis after cross-facial nerve grafting. Adipose-derived stem cell transplantation increased the number of axons that breach the coaptation site and enter the graft, optimized myelination to achieve maximal functional and structural efficiency, and supported the functional integrity of denervated neuromuscular junctions. We think that these beneficial effects are achieved mainly by the differentiation of adipose-derived stem cells into a Schwann cell-like phenotype, which promotes neurite outgrowth^{28–30} and myelination.^{31,32} In addition to their ability to differentiate, adipose-derived stem cells can secrete a plethora of growth factors that can mediate angiogenesis, wound healing, tissue regeneration, and immune cell reactions.^{33,34} In the context of the nervous system, it has been shown that adipose-derived stem cells produce a wide variety of

neurotrophic factors that can enhance neurite outgrowth and provide neuroprotection.^{35–37} However, the problems encountered in using a cross-facial nerve graft after facial paralysis to restore function, however, are more complex. Further studies are needed to determine the underlying mechanisms.

Ozan L. Abbas, M.D.

Department of Plastic, Reconstructive, and Aesthetic Surgery
Ahi Evran University
Faculty of Medicine
No 1, 2019th Street
Kırşehir, Turkey 40000
ozanluay@hotmail.com

ACKNOWLEDGMENT

This study was supported by the Baskent University Research Fund.

REFERENCES

- Melvin TA, Limb CJ. Overview of facial paralysis: Current concepts. *Facial Plast Surg.* 2008;24:155–163.
- Bascom DA, Schaitkin BM, May M, Klein S. Facial nerve repair: A retrospective review. *Facial Plast Surg.* 2000;16:309–313.
- Vlastou C. Facial paralysis. *Microsurgery* 2006;26:278–287.
- Faris C, Lindsay R. Current thoughts and developments in facial nerve reanimation. *Curr Opin Otolaryngol Head Neck Surg.* 2013;21:346–352.
- Boahene K, Byrne P, Schaitkin BM. Facial reanimation: Discussion and debate. *Facial Plast Surg Clin North Am.* 2012;20:383–402.
- Harrison DH. Current trends in the treatment of established unilateral facial palsy. *Ann R Coll Surg Engl.* 1990;72:94–98.
- Manktelow RT. Free muscle transplantation for facial paralysis. *Clin Plast Surg.* 1984;11:215–220.
- O'Brien BM, Pederson WC, Khazanchi RK, Morrison WA, MacLeod AM, Kumar V. Results of management of facial palsy with microvascular free-muscle transfer. *Plast Reconstr Surg.* 1990;86:12–22; discussion 23.
- Guntinas-Lichius O, Irintchev A, Streppel M, et al. Factors limiting motor recovery after facial nerve transection in the rat: Combined structural and functional analyses. *Eur J Neurosci.* 2005;21:391–402.
- Boyd JG, Gordon T. Glial cell line-derived neurotrophic factor and brain-derived neurotrophic factor sustain the axonal regeneration of chronically axotomized motoneurons in vivo. *Exp Neurol.* 2003;183:610–619.
- Schäffler A, Büchler C. Concise review: Adipose tissue-derived stromal cells. Basic and clinical implications for novel cell-based therapies. *Stem Cells* 2007;25:818–827.
- Gomillion CT, Burg KJ. Stem cells and adipose tissue engineering. *Biomaterials* 2006;27:6052–6063.
- di Summa PG, Kalbermatten DF, Pralong E, Raffoul W, Kingham PJ, Terenghi G. Long-term in vivo regeneration of peripheral nerves through bioengineered nerve grafts. *Neuroscience* 2011;181:278–291.
- di Summa PG, Kingham PJ, Raffoul W, Wiberg M, Terenghi G, Kalbermatten DF. Adipose-derived stem cells enhance peripheral nerve regeneration. *J Plast Reconstr Aesthet Surg.* 2010;63:1544–1552.

15. Dadon-Nachum M, Melamed E, Offen D. Stem cells treatment for sciatic nerve injury. *Expert Opin Biol Ther.* 2011;11:1591–1597.
16. Guntinas-Lichius O, Angelov DN, Tomov TL, Dramiga J, Neiss WF, Wewetzer K. Transplantation of olfactory ensheathing cells stimulates the collateral sprouting from axotomized adult rat facial motoneurons. *Exp Neurol.* 2001;172:70–80.
17. Jeronimo A, Jeronimo CA, Rodrigues Filho OA, Sanada LS, Fazan VP. Microscopic anatomy of the sural nerve in the postnatal developing rat: A longitudinal and lateral symmetry study. *J Anat.* 2005;206:93–99.
18. Komisaruk BR. Synchrony between limbic system theta activity and rhythmical behavior in rats. *J Comp Physiol Psychol.* 1970;70:482–492.
19. Wineski LE. Facial morphology and vibrissal movement in the golden hamster. *J Morphol.* 1985;183:199–217.
20. Kimura J. Principles and pitfalls of nerve conduction studies. *Ann Neurol.* 1984;16:415–429.
21. Kimura J. Facts, fallacies, and fancies of nerve conduction studies: Twenty-first annual Edward H. Lambert Lecture. *Muscle Nerve.* 1997;20:777–787.
22. Okajima Y, Toikawa H, Hanayama K, Ohtsuka T, Kimura A, Chino N. Relationship between nerve and muscle fiber conduction velocities of the same motor unit in man. *Neurosci Lett.* 1998;253:65–67.
23. Chomiak T, Hu B. What is the optimal value of the g-ratio for myelinated fibers in the rat CNS? A theoretical approach. *PLoS One.* 2009;4:e7754.
24. De Jaco A, Augusti-Tocco G, Biagioni S. Muscarinic acetylcholine receptors induce neurite outgrowth and activate the synapsin I gene promoter in neuroblastoma clones. *Neuroscience.* 2002;113:331–338.
25. Loreti S, Ricordy R, De Stefano ME, Augusti-Tocco G, Tata AM. Acetylcholine inhibits cell cycle progression in rat Schwann cells by activation of the M2 receptor subtype. *Neuron Glia Biol.* 2007;3:269–279.
26. Al-Majed AA, Neumann CM, Brushart TM, Gordon T. Brief electrical stimulation promotes the speed and accuracy of motor axonal regeneration. *J Neurosci.* 2000;20:2602–2608.
27. Gordon T, Brushart TM, Amirjani N, Chan KM. The potential of electrical stimulation to promote functional recovery after peripheral nerve injury: Comparisons between rats and humans. *Acta Neurochir Suppl.* 2007;100:3–11.
28. Kaewkhaw R, Scutt AM, Haycock JW. Anatomical site influences the differentiation of adipose-derived stem cells for Schwann-cell phenotype and function. *Glia.* 2011;59:734–749.
29. Jiang L, Zhu JK, Liu XL, Xiang P, Hu J, Yu WH. Differentiation of rat adipose tissue-derived stem cells into Schwann-like cells in vitro. *Neuroreport.* 2008;19:1015–1019.
30. Kingham PJ, Kalbermatten DF, Mahay D, Armstrong SJ, Wiberg M, Terenghi G. Adipose-derived stem cells differentiate into a Schwann cell phenotype and promote neurite outgrowth in vitro. *Exp Neurol.* 2007;207:267–274.
31. Xu Y, Liu L, Li Y, et al. Myelin-forming ability of Schwann cell-like cells induced from rat adipose-derived stem cells in vitro. *Brain Res.* 2008;1239:49–55.
32. Mantovani C, Mahay D, Kingham M, Terenghi G, Shawcross SG, Wiberg M. Bone marrow- and adipose-derived stem cells show expression of myelin mRNAs and proteins. *Regen Med.* 2010;5:403–410.
33. Salgado AJ, Reis RL, Sousa NJ, Gimble JM. Adipose tissue derived stem cells secretome: Soluble factors and their roles in regenerative medicine. *Curr Stem Cell Res Ther.* 2010;5:103–110.
34. Kapur SK, Katz AJ. Review of the adipose derived stem cell secretome. *Biochimie.* 2013;95:2222–2228.
35. Kalbermatten DF, Schaakxs D, Kingham PJ, Wiberg M. Neurotrophic activity of human adipose stem cells isolated from deep and superficial layers of abdominal fat. *Cell Tissue Res.* 2011;344:251–260.
36. Lattanzi W, Geloso MC, Saulnier N, et al. Neurotrophic features of human adipose tissue-derived stromal cells: In vitro and in vivo studies. *J Biomed Biotechnol.* 2011;2011:468705.
37. Chung JY, Kim W, Im W, et al. Neuroprotective effects of adipose-derived stem cells against ischemic neuronal damage in the rabbit spinal cord. *J Neurol Sci.* 2012;317:40–46.